Determination of the Time Evolution of Fission from Particle Emission

J. P. Lestone
Los Alamos National Laboratory, Los Alamos, New Mexico 87545
(Received 14 December 1992)

Recently measured properties of the prescission particle emission from heavy-ion induced fission of systems with $A \sim 200$ were analyzed using the statistical model. Simultaneous fits to prescission neutron, proton, and α-particle multiplicities and mean kinetic energies can be obtained when the deformation dependence of both the particle transmission coefficients and particle binding energies are taken into account. The experimental data are consistent with a total fission time scale of $(30 \pm 10) \times 10^{-21}$ s, with more than half of this time being spent beyond the saddle point.

PACS numbers: 25.70.Jj, 25.85.Ge

The determination of the nature and magnitude of nuclear dissipation and its effects on the fission process has, for the last decade, remained a topic of great interest. The slowing of the fission process due to nuclear dissipation manifests itself as an excess of prescission neutrons [1,2], light charged particles [3,4], and electric-dipole γ rays [5,6], relative to predictions from standard statistical model codes [7–9]. These results imply that nuclear dissipation is high and that movement in the fission direction is overdamped.

One possible method of incorporating the delaying effects of nuclear dissipation into statistical model calculations [4] is to allow only particle emission from nearly spherical systems for a time τ_{pre} (the presaddle delay time) and then allow the fission decay to compete with the particle emission. The presaddle delay τ_{pre} is related to the transient time τ_{tr} required to establish the quasiequilibrium population at the saddle point [10]. The evaporation of particles during the descent from saddle to scission can be modeled by considering particle emission from a system with a deformation somewhere between the saddle and scission points, for a time τ_{ssc} (the saddle-to-scission transition time). The total fission time scale can be defined as $\tau_{total} = \tau_{pre} + \tau_{ssc}$.

Hinde *et al.* [2] recently analyzed prescission neutron multiplicities ν_{pre} and mean neutron kinetic energies E_ν. They extracted a total fission time scale of $\tau_{total} = (35 \pm 15) \times 10^{-21}$ s. Their analysis gives no information on the breakup of this total fission time scale into a presaddle delay and a saddle-to-scission transition time. Since the effective Coulomb emission barriers for proton and α-particle emission decrease with deformation, it should be possible to use light charged particle emission to better define the time evolution of fissioning systems. Measured prescission neutron, proton, and α-particle multiplicities from the fission of the compound nuclei ^{192,195,198}Pb, formed in Er+Si reactions, were recently analyzed [4] using an early version of the statistical model code JOANNE [9]. The findings of this work were that τ_{pre} is limited to $\lesssim 10 \times 10^{-21}$ s and that the neutron emission originates predominantly from nuclei with deformations significantly larger than the equilibrium value. Although this early version of JOANNE incorporated a presaddle delay and a saddle-to-scission transition time, it made two very simplifying assumptions. The particle transmission coefficients T_l were assumed to be independent of deformation, and the thermal excitation energies and particle binding energies during the descent from saddle to scission were taken to be equal to the average of those at the saddle and scission points. These assumptions meant that the information contained in the kinetic energies of the prescission protons and α particles could not be used to determine the time evolution of the fissioning systems and that the extracted τ_{ssc} could not be trusted.

For this Letter we use the latest version of JOANNE which does not make the simplifying assumptions mentioned above. The presaddle particle decay widths were calculated using rotating finite range model [11] (RFRM) deformation plus rotational energies, liquid drop model [12] (LDM) particle binding energies and T_l's obtained using universal optical model potentials [13,14]. The statistical model fission widths were determined using RFRM fission barriers. To enable the determination of the saddle-to-scission particle decay widths, one must first choose a deformation of the nucleus somewhere between the values at the saddle and scission points. Factors influencing the particle decay widths as a function of deformation, such as shape and deformation energy, were determined using axially symmetric nuclear shapes and the rotating liquid drop model (RLDM) [15]. To obtain the particle transmission coefficients for the deformed saddle-to-scission emitter, we used a simple approximate procedure similar to that of Ref. [16]. The radii of the nuclear optical potentials [13,14] were varied as a function of the angle to the symmetry axis determined by RLDM nuclear shapes. The Coulomb potentials around the deformed nuclei were determined using the results of Ref. [17]. These transmission coefficients predict a decrease in the effective proton and α-particle emission barriers with increasing deformation. Figure 1 shows the change in the mean kinetic energy of neutrons, protons, and α particles from ^{195}Pb compound nuclei with $J = 0$ and $E^* = 50$ MeV as a function of the elongation of the symmetry axis Z_{axis} (in units of the diameter of the

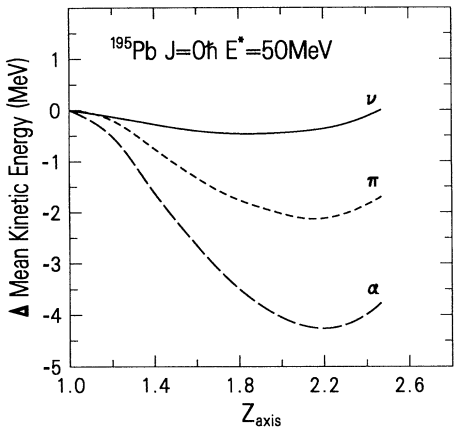

FIG. 1. Change in the mean kinetic energies of neutrons, protons, and α particles from ^{195}Pb compound nuclei with $J=0$ and $E^*=50$ MeV as a function of the elongation of the symmetry axis Z_{axis} (in units of the diameter of the spherical system) relative to the emission from spherical nuclei.

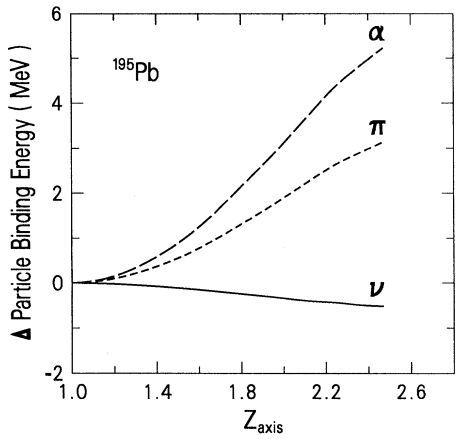

FIG. 2. Change in neutron, proton, and α-particle binding energies as a function of Z_{axis} relative to the spherical binding energies for ^{195}Pb compound nuclei.

spherical system), relative to the emission from spherical nuclei. The small changes in the mean neutron energies are due to the dependence of the deformation energy on Z_{axis}. The initial decrease in the mean kinetic energy of the light charged particle emission is mainly due to changes in the T_l's. The increase above $Z_{axis}\sim 2.2$ is due to the rapid rise in the thermal excitation energy as the scission point is approached. The decrease in the effective proton and α-particle emission barriers gives an enhancement of the charged particle emission relative to the neutron emission. Many people thus expect a favoring of charged particle emission with increasing deformation. However, when modeling particle emission from deformed nuclei, the dependence of the particle binding energies on deformation must be taken into account. Particle binding energies as a function of deformation can be written as

$$B_{\rm part}=M_{\rm part}+M_d^s+D_d(\alpha_i)-M_p^s-D_p(\alpha_i)\,,$$

where $M_{\rm part}$ is the mass of the emitted particle, M_d^s and M_p^s are the masses of the spherical daughter and parent nuclei, respectively. D_d and D_p are the deformation energies of the daughter and parent nuclei, which are functions of the nuclear shape as specified by parameters α_i. The LDM particle binding energies for neutron, proton, and α-particle emission from ^{195}Pb are 8.2, 3.4, and -5.4 MeV, respectively. Figure 2 shows the change in these binding energies as a function of the elongation of the symmetry axis Z_{axis}. The neutron binding energies decrease slightly while the proton and α-particle binding energies increase dramatically with deformation. Such behavior is expected, since for a fixed deformation the removal of charge causes a rapid increase in nuclear deformation energy, while the removal of neutrons causes a slight decrease. The increase in the light charged particle binding energies causes a suppression of the proton and α-particle emission with increasing deformation. For systems with $A\sim 200$ this suppression of the charged particle emission is greater than the enhancement associated with the drop in the effective emission barriers. Thus for $A\sim 200$ the model presented here predicts a suppression of the charged particle emission relative to the neutron emission with increasing deformation. Without this suppression, it would not be possible to obtain the simultaneous fits to the prescission neutron, proton, and α-particle multiplicities ($\nu_{\rm pre}$, $\pi_{\rm pre}$, and $\alpha_{\rm pre}$) and mean kinetic energies (E_ν, E_π, and E_α) shown later.

Figure 3 shows combinations of $\tau_{\rm pre}$ and $\tau_{\rm ssc}$, which individually reproduce the measured values [4,9] of $\alpha_{\rm pre}=0.074\pm 0.005$, $E_\alpha=20.5\pm 0.3$ MeV, $\pi_{\rm pre}=0.107\pm 0.009$ and $E_\pi=11.5\pm 0.2$ MeV for the reaction ^{164}Er +185 MeV ^{28}Si$\rightarrow$ ^{192}Pb. These calculations were per-

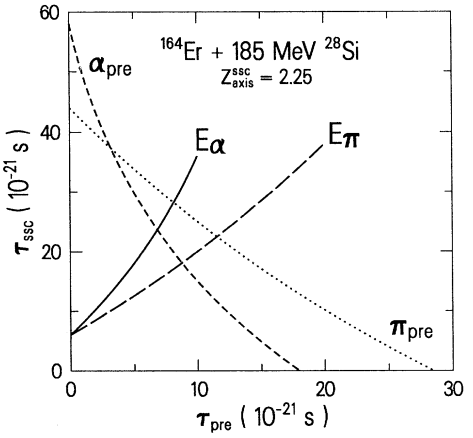

FIG. 3. Combinations of $\tau_{\rm pre}$ and $\tau_{\rm ssc}$, which individually reproduce the experimental values [4,9] of $\pi_{\rm pre}$, $\alpha_{\rm pre}$, E_π, and E_α for the reaction ^{164}Er+ 185 MeV ^{28}Si$\rightarrow$ ^{192}Pb.

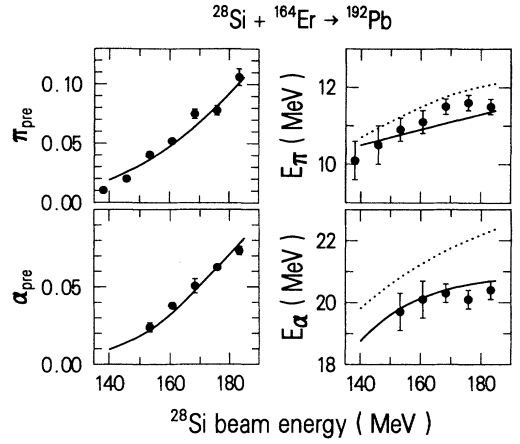

FIG. 4. Comparison of measured τ_{pre}, α_{pre}, E_π, and E_α for the reaction $^{164}Er+{}^{28}Si \rightarrow {}^{192}Pb$ to calculations using $\tau_{pre}=9\times10^{-21}$ s, $\tau_{ssc}=22\times10^{-21}$ s, and a_ν based on the theoretical values of Ref. [18] (solid lines). The dotted lines show the calculated E_π and E_α assuming emission only from spherical systems.

formed using level density parameters $a_\nu(A,a_i)$ based on the theoretical values of Ref. [18], an elongation of the saddle-to-scission emitter of $Z^{ssc}_{axis}=2.25$, and values of a_f/a_ν adjusted to reproduce the experimental evaporation-residue cross section [19]. The elongation of the saddle-to-scission emitter of $Z^{ssc}_{axis}=2.25$ corresponds to a deformation approximately half way between the saddle and scission points. Similar analyses were performed using various other values for the elongation of the saddle-to-scission emitter. It was found that the extracted values of τ_{pre} and τ_{ssc} were insensitive to Z^{ssc}_{axis}. $\tau_{pre}\sim9\times10^{-21}$ s and $\tau_{ssc}\sim22\times10^{-21}$ s were found to give simultaneous fits to the prescission proton and α-particle data, independent of the deformation chosen for the saddle-to-scission emitter. Figure 4 compares calculations to the measured values of π_{pre}, α_{pre}, E_π, and E_α for the reaction $^{164}Er+{}^{28}Si$ as a function of the ^{28}Si beam energy. Similar agreement between model and experiment is found for the $^{167,170}Er+{}^{28}Si$ reactions [4,9], and with recently measured prescission light charged particle multiplicities for the $^{181}Ta+{}^{19}F$ reaction [20].

Unlike the calculations of the properties of the prescission light charged particles, calculations of ν_{pre} are very sensitive to the elongation of the symmetry axis of the saddle-to-scission emitter. In order to obtain an estimate of the deformation of the saddle-to-scission emitter, calculations of ν_{pre} as a function of Z^{ssc}_{axis} were compared to five recent measurements of prescission neutron multiplicities [2] for fusion-fission reactions with $A\sim200$ and $E^*\sim100$ MeV. Acceptable fits to the ν_{pre} data are obtained with $Z^{ssc}_{axis}=2.21\pm0.06$. Table I compares measured values of ν_{pre} and E_ν [2] to calculations using $Z^{ssc}_{axis}=2.21$. Although the deformation of the saddle-to-scission emitter was adjusted only to reproduce the measured ν_{pre}, the agreement with E_ν is also excellent. The uncertainties in the measured E_ν can be used to place limits on the level density parameters. It was found that the measured E_ν imply a_ν is within 6% of the theoretical values of Ref. [18]. This uncertainty in $a_\nu(A,a_i)$ and the experimental uncertainties in the properties of the prescission proton and α-particle emission lead to the following uncertainties in the fission times scales: $\tau_{pre}=(9\pm6)\times10^{-21}$ s and $\tau_{ssc}=(22\pm7)\times10^{-21}$ s. For compound nuclei $A\sim200$, $E^*\sim100$ MeV, these values imply that $\sim60\%$ of the neutron emission and $\sim40\%$ of the light charged particle emission occur during the descent from saddle to scission.

TABLE I. Comparison of experimental values of ν_{pre} and E_ν [2] to those calculated using $\tau_{pre}=9\times10^{-21}$ s, $\tau_{ssc}=22\times10^{-21}$ s, $Z^{ssc}_{axis}=2.21$, and a_ν based on the theoretical values of Ref. [18].

Reaction	ν_{pre} Expt.	Cal.	E_ν (MeV) Expt.	Cal.
^{141}Pr+249 MeV ^{40}Ar	2.65 ± 0.30	2.2	3.58 ± 0.20	3.5
^{169}Tm+159 MeV ^{18}O	3.70 ± 0.30	3.7	3.56 ± 0.12	3.6
^{165}Ho+249 MeV ^{40}Ar	2.85 ± 0.30	3.1	3.37 ± 0.20	3.4
^{169}Tm+249 MeV ^{40}Ar	3.00 ± 0.30	2.9	3.34 ± 0.30	3.5
^{197}Au+159 MeV ^{18}O	4.10 ± 0.15	4.1	3.35 ± 0.08	3.4

In summary, we have presented a model which contains a presaddle delay τ_{pre}, a saddle-to-scission transition time τ_{ssc} and an elongation of the saddle-to-scission emitter Z^{ssc}_{axis} as free parameters. It was shown that values of these parameters can be chosen that lead to a simultaneous reproduction of prescission neutron, proton, and α-particle multiplicities and mean kinetic energies, from heavy-ion induced fission of systems with $A\sim200$. The deformation dependence of both the particle transmission coefficients and particle binding energies has to be taken into account when performing these calculations. The chosen values of τ_{pre}, τ_{ssc}, and Z^{ssc}_{axis} imply a total fission time scale of $(30\pm10)\times10^{-21}$ s with more than half of this time being spent beyond the saddle point.

[1] A. Gavron *et al.*, Phys. Rev. C **35**, 579 (1987).
[2] D. J. Hinde *et al.*, Phys. Rev. C **45**, 1229 (1992).
[3] G. F. Peaslee *et al.*, Phys. Rev. C **38**, 1730 (1988).
[4] J. P. Lestone *et al.*, Phys. Rev. Lett. **67**, 1078 (1991); J. P. Lestone *et al.* (to be published).
[5] R. Butsch *et al.*, Phys. Rev. C **44**, 1515 (1991).
[6] I. Diószegi *et al.*, Phys. Rev. C **46**, 627 (1992).
[7] M. Blann and T. T. Komoto, Phys. Rev. C **26**, 472 (1982).
[8] A. Gavron, Phys. Rev. C **21**, 230 (1980).
[9] J. P. Lestone, Ph.D. thesis, Australian National University, 1990, and Internal Report No. ANU/P1084 (unpublished).
[10] P. Grangé *et al.*, Phys. Rev. C **27**, 2063 (1983).

[11] A. J. Sierk, Phys. Rev. C **33**, 2039 (1986).
[12] W. D. Myers and W. J. Swiatecki, Nucl. Phys. **81**, 1 (1966).
[13] C. M. Perey and F. G. Perey, At. Data Nucl. Tables **17**, 1 (1976).
[14] J. R. Huizenga and G. Igo, Nucl. Phys. **29**, 462 (1962).
[15] S. Cohen *et al.*, Ann. Phys. (N.Y.) **82**, 557 (1974).
[16] J. R. Huizenga *et al.*, Phys. Rev. C **40**, 668 (1989).
[17] K. T. R. Davies and J. R. Nix, Phys. Rev. C **14**, 1977 (1976).
[18] J. Töke and W. J. Swiatecki, Nucl. Phys. **A372**, 141 (1981).
[19] D. J. Hinde *et al.*, Nucl. Phys. **A398**, 308 (1983).
[20] H. Ikezoe *et al.*, Phys. Rev. C **46**, 1922 (1992).